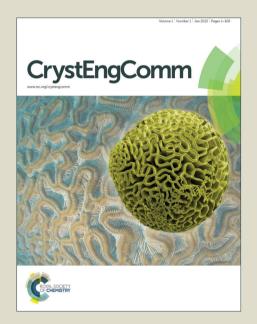# CrystEngComm

This is an *Accepted Manuscript*, which has been through the Royal Society of Chemistry peer review process and has been accepted for publication.

Accepted Manuscripts are published online shortly after acceptance, before technical editing, formatting and proof reading. Using this free service, authors can make their results available to the community, in citable form, before we publish the edited article. We will replace this *Accepted Manuscript* with the edited and formatted *Advance Article* as soon as it is available.

You can find more information about *Accepted Manuscripts* in the **Information for Authors**.

CrystEngComm

ARTICLE

Achieving single domain relaxor-PT crystals by high temperature poling

Fei Li[a], Linghang Wang[a], Li Jin[a], Zhuo Xu[a], and Shujun Zhang[*b]

Single domain relaxor-PT crystals are important from both fundamental and application viewpoints. Compared to domain engineered relaxor-PT crystals, however, single domain crystals are prone to crack during poling. In this paper, based on the analysis of the cracking phenomenon in [001] poled tetragonal $0.25Pb(In_{0.5}Nb_{0.5})O_3$-$0.37Pb(Mg_{1/3}Nb_{2/3})O_3$-$0.38PbTiO_3$ (PIN-PMN-PT) crystals, the non-180° ferroelastic domain switching was thought to be the dominant factor for the cracks during poling process. A high temperature poling technique, by which the domain switching can be greatly avoided, was proposed to achieve the single domain relaxor-PT crystals. By this poling approach, a quasi-single domain crystal was obtained without cracks. In addition, compared to room temperature poling, the high temperature poled PIN-PMN-PT crystals showed improved electromechanical properties, i.e., low dielectric loss, low strain-electric field hysteresis and high mechanical quality factor, demonstrating a beneficial poling approach.

1. Introduction

Relaxor-$PbTiO_3$ (Relaxor-PT) based ferroelectric single crystals, such as $Pb(Mg_{1/3}Nb_{2/3})O_3$-$PbTiO_3$ (PMN-PT) and $Pb(In_{1/2}Nb_{1/2})O_3$-$Pb(Mg_{1/3}Nb_{2/3})O_3$-$PbTiO_3$ (PIN-PMN-PT), have attracted considerable interest, because of their ultrahigh piezoelectric activities, far outperforming the state-of-art polycrystalline $Pb(Zr,Ti)O_3$ (PZT) ceramics.[1-6] Over the last decade, extensive studies have been focused on the piezoelectric response of domain engineered crystals, especially for [001] poled rhombohedral relaxor-PT crystals, with longitudinal piezoelectric coefficient d_{33} and electromechanical coupling factor k_{33} being on the order of >1500 pC/N and > 0.9, respectively. Ferroelectric phase instability is thought to be responsible for the high piezoelectric activity in relaxor-PT crystals,[7-8] which can be induced by the phase transition points (for example, morphotropic phase boundary and polymorphic phase transition) and relaxor component.[2] In addition to the high piezoelectric response, hysteresis-free strain-electric field behavior is another important characteristic for relaxor-PT crystals, which inherently associated with the engineered domain

configuration. In rhombohedral (R) crystals, there are eight degenerate domain variants, with the polar vectors (spontaneous polarizations) along one of the <111> directions. As R crystal is poled along the non-polar [001] direction, four of the eight domain variants are energetically favored by the poling field, with polar vectors along $[111], [\bar{1}11], [1\bar{1}1]$, and $[11\bar{1}]$ directions. This domain structure is labelled as "4R".[9] Because these four domain variants are equivalent to the poling [001] direction, the domain structure is stable as the electric field is applied along [001] direction, resulting in a hysteresis-free strain-electric field response.[1] Similarly, [001] poled orthorhombic and [111] poled tetragonal relaxor-PT crystals possess "4O" and "3T" domain engineered configurations respectively[9], which exhibit hysteresis-free strain characteristics. Thus, domain engineered relaxor-PT crystals greatly benefit the piezoelectric transducer and actuator applications.[10-12]

Compared to the domain engineered crystals, single domain relaxor-PT crystals, though not received much attention, are important in both aspects of science and application. In scientific aspect, the data of the single domain crystals is essential for studying domain engineered crystals and polycrystalline ceramics. Based on the single domain data, the intrinsic piezoelectric response of crystals (regardless of domain wall motion) and the anisotropy of the crystal properties can be derived.[2,13-14] From application viewpoint, on the other hand, single domain crystals exhibit many advantages, such as high thickness shear piezoelectric and pyroelectric properties.[15-21] As given in Table I,[2, 15] the shear piezoelectric activities of single domain crystals are much higher than those

[a] Electronic Materials Research Laboratory, Key Laboratory of the Ministry of Education and International Center for Dielectric Research, Xi'an Jiaotong University, Xi'an 710049, China

[b] Materials Research Institute, Pennsylvania State University, University Park, Pennsylvania 16802, USA. Email: soz1@psu.edu.

of domain engineered crystals, with d_{15} and k_{15} being on the order of ~2000 pC/N and >90%, respectively. In addition, compared with the longitudinal piezoelectric response of domain engineered crystals, shear piezoelectric response of single domain crystals can be used in the condition of high preload stress. Preload stress may induce phase transition and depoling in domain engineered crystals,[22-25] while the thickness shear mode of single domain crystals was found to be stabilized upon the preload stress.[26] Of particular significance is that the shear piezoelectric coefficient d_{24} of single domain orthorhombic crystals was found to maintain similar value at temperature of -50 °C~100 °C (the T_{OT} phase transition temperature), with variation being around 6%,[27] while the longitudinal piezoelectric coefficient d_{33} of [001] poled rhombohedral crystals generally exhibit 200-300% variation in the same temperature range. [2] These advantages make single domain relaxor-PT crystals good candidates for various shear mode applications, such as vector sensors, non-destructive evaluation (NDE) transducers and low frequency acoustic transducers. Nevertheless, single domain crystals subject to cracking from the electric-field-induced strain/stress during the poling process. Thus, it is desirable to investigate the poling procedure and understand the underlying crack mechanism.

To obtain domain engineered configurations, the ferroelectric crystals are poled along specific non-polar directions, so various domains appear in the crystals. These domains can form various non-180° domain configurations, satisfying the mechanical compatibility to minimize the strain energy.[28-29] For single domain crystals, however, the strain energy cannot be released by the non-180° domains. With the poling electric field applied along spontaneous polar direction (to achieve single domain state), the crystals will release the strain energy from alternative way, i.e., cracking. Therefore, practically it is hard to get a crack-free single domain relaxor-PT ferroelectric crystal, which hinders the investigation and application of single domain crystals. In this paper, we compared the strain-electric field behaviors of domain engineered and single domain $0.25Pb(In_{0.5}Nb_{0.5})O_3$-$0.37Pb(Mg_{1/3}Nb_{2/3})O_3$-$0.38PbTiO_3$ (PIN-PMN-PT) tetragonal crystals and analyzed the cracking phenomenon during the poling procedure. Then, we proposed a high temperature poling technique to get crack-free single domain crystals. Finally, we compared the electromechanical properties of room temperature poled and high temperature poled crystals.

2. Samples preparation and measurements

The PIN-PMN-PT crystals were grown using the modified Bridgman technique at XJTU.[30] The composition of crystal was determined by electron probe X-ray microanalyzer (EPMA). The Curie temperature and coercive field were found to be 215 °C and 10 kV/cm, respectively. The lattice parameter c/a ratio was measured by X-ray diffraction (XRD RIGAKU D/MAX-2400), being on the order of 1.015. The crystals were oriented by RO-XRD method [31-32] and cut to obtain the samples with various dimensions (thickness-mode plates, longitudinal rods, and thickness shear-mode plates) for measuring the electromechanical properties following IEEE standard.[33] Vacuum sputtered gold was applied to the polished surface as the electrodes for all the samples. The impedance-frequency behaviors were determined using an HP4294 impedance analyzer. Strain-electric field behaviors were determined using a linear variable differential transducer (LVDT) driven by a lock-in amplifier (Stanford Research system, Mode SR830). A polarizing light microscope (PLM) with a 0°/90° crossed polarizer/analyzer (P/A) pair (Olympus BX51) was used to observe the extinction behavior of the poled samples.

3. Poling method

To facilitate the domain switching process, ferroelectric ceramics, such as PZT ceramics, are poled at elevated temperature, which is higher than room temperature but much lower than the Curie temperature, being about 100-150 °C. On the contrary, the relaxor-PT crystals are generally poled at room temperature, because the coercive fields E_c of these crystals are very low, being 2-5 kV/cm (E_c of PZT ceramics is in the range of 10-40 kV/cm). In practice, to obtain domain engineered structure, relaxor-PT crystals are poled at room temperature by an electric field of two-fold of E_c along their nonpolar directions. However, the crystals are prone to crack and lots of domain walls yet exist when poled along polar direction at room temperature.

Table I. Comparison of shear piezoelectricity and pyroelectric response among domain engineered crystals ([001] poled PMN-0.30PT crystal) and single domain crystals. Coefficients $\varepsilon_{11}^T/\varepsilon_{22}^T$, s_{55}^E/s_{44}^E, d_{15}/d_{24}, and p are dielectric, elastic, piezoelectric and pyroelectric coefficients respectively.

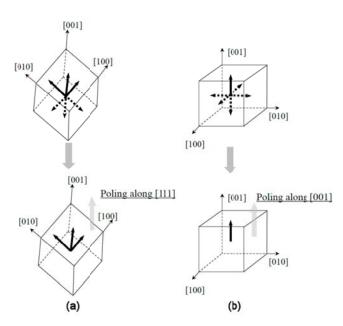| Materials	$\varepsilon_{11}^T/\varepsilon_0$	s_{55}^E (pm²/N)	d_{15} (pC/N)	$\varepsilon_{22}^T/\varepsilon_0$	s_{44}^E (pm²/N)	d_{24} (pC/N)	p (10^{-4} C/m²K)
[001] poled PMN-0.30PT crystals	1600	14.0	150	1600	14.0	150	4-6
Single domain rhombohedral Crystal	5000-8000	200-250	3000-5000	5000-8000	200-250	3000-5000	10-13
Single domain tetragonal Crystal	12000-18000	40-60	1800-2200	12000-18000	45-60	1800-2200	7-10
Single domain orthorhombic Crystal	5000-7000	200-320	3500-4500	12000-18000	45-60	1800-2200	/

Fig. 1 Domain evolution of tetragonal crystals during the poling process. (a) Poled along the [111] direction for "3T" domain engineered configuration; (b) poled along the [001] direction to obtain single domain crystal. The thick-black arrows represent the possible domain directions.

In order to design a poling method for obtaining crack-free single domain crystals, the domain evolution of tetragonal crystals are analyzed, by poling along [001] and [111] directions, respectively. For tetragonal relaxor-PT crystals, six different domains, i.e., along [001], [010], [100], $[\bar{1}00]$, $[0\bar{1}0]$, and $[00\bar{1}]$ directions, coexist prior to the poling process. As the crystal is poled along [111] direction, domains along $[\bar{1}00]$, $[0\bar{1}0]$, and $[00\bar{1}]$ directions transform to the other three electrically favored domains, forming engineered domain configuration "3T", as shown in Fig. 1(a). During the poling process, the electric-field-induced strain by domain switching is minimal, due to the spontaneous strain of these six domains are equivalent with respect to [111] direction. On the contrary, as the crystal is poled along polar [001] direction, the domains along [010], [100], $[\bar{1}00]$, $[0\bar{1}0]$, and $[00\bar{1}]$ directions transform to the [001] domain, as shown in Fig. 1(b). At this condition, the electric-field-induced strain is significantly large and abrupt, due to the ferroelastic 90° domain switching from [010], [100], $[\bar{1}00]$ or $[0\bar{1}0]$ domains to [001] domain.

Figure 2 shows the strain-electric field behaviors for [001] and [111] oriented tetragonal PIN-PMN-PT crystals. When the applied field is around E_c, six possible domains exist in the crystal, which can be regarded as the crystal state prior to poling. At high electric field section, only the domains with the direction closest to poling direction exist, which is the crystal state after poling. As expected, for [001] oriented crystals the negative strain is found to be 0.7%, with a sharp strain-electric field behavior at E_c, being attributed to the 90° domain switching. While the negative strain of [111] oriented crystals was only 0.08%, which is mainly contributed by the linear piezoelectric effect, being equal to $-d_{33}E_c$. It is interesting to note that if all the domains are along [010], $[0\bar{1}0]$, [100], or

$[\bar{1}00]$ directions before poling, the contribution of 90° domain switching to the strain should be equal to the ratio of $(c-a)/a$=1.5% (c and a are the lattice parameters). However, the reality is that before poling some domains are along [001] and $[00\bar{1}]$ directions, which can explain that the contribution of 90° domain switching to the strain is lower than the ratio of $(c-a)/a$ in [001] oriented tetragonal crystal.
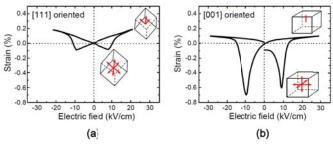

Fig. 2 The Strain-Electric field behaviors of (a) [111] and (b) [001] oriented tetragonal 0.25PIN-0.37PMN-0.38PT crystals, where the possible domains at different electric fields are shown by the red arrows. At coercive field, six possible domains appear in the crystal, which can be regarded as the crystal state prior to poling. At high electric field section, only the domains closest to poling direction exist, which is the state of crystal after poling.

According to the above discussion, the large strain variation is thought to be the dominant factor for the crack phenomenon when the crystals transform into single domain state. The large strain is induced by the ferroelastic domain switching (i.e., non-180° ferroelectric domain switching), which should be avoided during the poling process, in order to reduce the cracking. Based on this idea, a high temperature poling approach is proposed to obtain single domain crystals. As described in Figure 3, first the crystal was heated to the temperature above Curie temperature (from room temperature to 250°C at the rate of 5°C/min). Then, an electric field of 2~3 kV/cm was applied to [001] oriented tetragonal crystal. Finally, the crystal was slowly cooled down to room temperature with the applied dc electric field at the rate of 2°C/min. During this poling process, only the domain along [001] direction is expected to form through the paraelectric-ferroelectric phase transition point (T_C). Meanwhile, in this process the rate of strain change can be controlled by the temperature decreasing rate. Compared with the room-temperature poling process, therefore, 90° domain switching and abrupt strain variation are precluded in the above poling process.
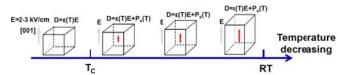
CrystEngComm Accepted Manuscript

Fig. 3 Schematic diagram of high temperature poling technique. The electric displacement is expressed at various temperatures. The red arrows represent the spontaneous polarization for tetragonal crystal. At the temperature high than T_c, the crystal is in paraelectric phase, where the spontaneous polarization and ferroelectric domains cannot be induced by electric field and the electric displacement only comes from linear dielectric response, being equal to $\varepsilon(T)E$. As the temperature decreases below T_c, the spontaneous polarization along the direction of electric field ([001] direction) will appear, and the electric displacement can be expressed as $\varepsilon(T)E+P_s(T)$. With further decreasing the temperature, the spontaneous polarization and strain increase gradually.

4. Comparison of tetragonal PIN-PMN-PT single domain crystals poled by general method (room temperature poling) and high temperature poling method

Figures 4(a1) and (b1) give the images of tetragonal PIN-PMN-PT crystals poled by room-temperature and high-temperature techniques, respectively. High density of domain walls and cracks were observed in the room-temperature poled crystals, while the high temperature poled crystals do not show any cracks. It should be noted that some domain walls still present around the surface of the high temperature poled crystal. These domain walls are hard to be removed, because the applied electric field near the surface deviate a lot from the ideal situation, i.e., the direction of the applied electric field is not strictly parallel to [001] direction on the proximity of sample surface. Figures 4(a2) and (b2) show the PLM images of [001] poled tetragonal PIN-PMN-PT, where the light propagate along [100] direction, the polarizer and analyser are set along [010] and [001] directions, respectively. In principle, six possible domains of tetragonal crystal should exhibit extinction as the polarized-light propagates along [100] direction with polarizer/analyzer being along [010]/[001] directions.[34] However, due to the influence of high density of domain walls (the symmetry of domain wall is lower than that of tetragonal domain[35-36]), room-temperature poled crystal does not show extinction phenomenon, again indicating that the density of domain walls in room-temperature poled crystals is much higher than that in high temperature poled counterpart.

Table II shows the electromechanical properties for longitudinal mode tetragonal PIN-PMN-PT crystals. Although the dielectric permittivity, piezoelectric coefficient and coupling factor are similar for room temperature and high temperature poled crystals, the dielectric and mechanical losses, which are mainly attributed to domain wall motion,[37-40] are much higher for the room-temperature poled crystals.
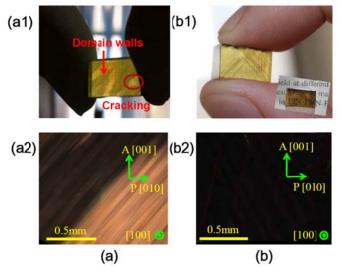

Fig. 4 Images for 0.25PIN-0.37PMN-0.38PT crystals poled by (a) room-temperature and (b) high-temperature techniques, respectively. Figures (a1) and (b1) were taken by camera. Figures (a2) and (b2) were taken by a polarizing light microscope with a 0°/90° crossed polarizer/analyzer (P/A) pair. In these pictures, the dimension of the samples is 6 mm ([100])×12 mm ([010])×8 mm ([001]). The samples are poled along polar [001] direction, and the (100) surfaces are optical polished for domain observation.
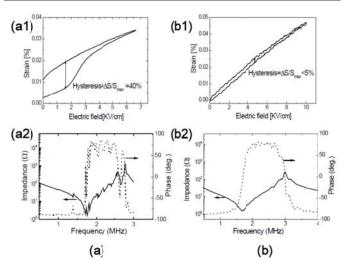

Fig. 5 Electromechanical properties for [001] oriented 0.25PIN-0.37PMN-0.38PT crystals poled by (a) room-temperature and (b) high-temperature techniques respectively. Figures (a1) and (b1) are unipolar strain-electric field response. Figures (a2) and (b2) are impedance and phase spectrum of thickness shear mode. The longitudinal rods with dimension of 5 mm (poling direction)×1.5 mm ×1.5 mm are used for strain-electric field measurements. The shear thickness plates with dimension of 5 mm (poling direction)×5 mm×0.5 mm are used for measuring the impedance and phase spectrum of 15-mode. The shear piezoelectric coefficients d_{15} of room-temperature and high temperature poled crystal are 1800 and 2000 pC/N respectively.

CrystEngComm

ARTICLE

Table II. Longitudinal electromechanical properties of [001] poled tetragonal 0.25PIN-0.37PMN-0.38PT crystals. Plate samples with dimension of 10 mm× 10 mm×1 mm (poling direction) were used for measuring the dielectric permittivity and loss. Longitudinal rods with dimension of 8 mm (poling direction)× 2 mm×2 mm were used for measuring the d_{33}, k_{33} and mechanical quality factor. Mechanical quality factor Q_m is the inverse of mechanical loss.

Materials	Dielectric permittivity $\varepsilon_{33}^T/\varepsilon_0$	Piezoelectric coefficient d_{33} (pC/N)	Coupling factor k_{33}	Dielectric loss tanδ	Mechanical quality factor Q_m
Room temperature poled crystal	1100-1400	450-480	83%	0.5-2%	300-700
High temperature poled crystal	1000-1200	450-470	84%	0.1-0.3%	1500-2500

The effects of incomplete poling and domain walls are more obvious in the strain-electric field and impedance-frequency behaviors for the tetragonal PIN-PMN-PT crystals. As shown in Fig. 5(a1) and (b1), a nearly linear strain-electric field response was observed for high temperature poled crystals, while a large strain hysteresis (~40%) induced by the domain wall motion was shown in room-temperature poled counterpart. Figure 5(a2) and (b2) show the impedance and phase spectra for thickness shear vibration mode (15-mode). The clean shear-mode resonance and antiresonance peaks were observed in high temperature poled crystal. For room-temperature poled crystal, however, some other vibrations (i.e., thickness vibration) might be coupled with the thickness shear-mode, because the domains along [100] or [010] directions yet exist. Meanwhile, the homogeneity of electromechanical properties may be affected by uneven distribution of domains and domain walls in the room-temperature poled crystal, as depicted in Fig. 4(a1). Due to the above two factors, noisy impedance-peaks were observed in the room-temperature poled samples. The large strain hysteresis and noisy peaks of the room temperature poled piezoelectric crystals can greatly restrict their electromechanical applications.

5. Conclusions

The [001] and [111] oriented 0.25PIN-0.37PMN-0.38PT tetragonal crystals poled at different conditions were investigated, the underlying mechanism of the cracks in single domain crystals was attributed to the large strain variation induced by ferroelastic domain switching. A feasible high temperature poling technique was proposed, by which, a quasi-single domain tetragonal PIN-PMN-PT crystal was obtained without cracks. Compared to the room-temperature poled crystals, high temperature poled crystals exhibited a low density of domain walls, leading to greatly reduced dielectric loss, strain hysteresis and increased mechanical quality factor, without sacrificing the piezoelectric properties. The proposed method may also benefit other perovskite ferroelectric crystals for achieving single domain state, such as barium titanate and potassium-sodium niobate crystals.

References

1. S. E. Park and T. R. Shrout, *J. Appl. Phys.*, 1997, **82**, 1804.
2. S. Zhang and F. Li, *J. Appl. Phys.*, 2012, **111**, 031301.
3. X. Li and H. Luo, *J. Am. Ceram. Soc.*, 2010, **93**, 2915.
4. N. Luo, Y. Li, Z. Xia, and Q. Li, *CrystEngComm*, 2012, **14**, 4547.
5. F. Li, S. Zhang, Z. Xu, X. Wei, and T. R. Shrout, *J. Appl. Phys.*, 2011, **109**, 014108.
6. G . S. Xu, K. Chen, D. F. Yang, and J. B. Li, *Appl. Phys. Lett.*, 2007, **90**, 032901.
7. D. Damjanovic, *IEEE Trans. Ultrason. Ferroelectr. Freq. Control*, 2009, **56**, 1574.
8. F. Li, S. Zhang, Z. Xu, X. Wei, J. Luo, T. R. Shrout, *J. Appl. Phys.*, 2010, **108**, 034106.
9. M. Davis, D. Damjanovic, D. Hayem, and N. Setter, *J. Appl. Phys.*, 2005, **98**, 014102.
10. X. Jiang, P. W. Rehrig, W. S. Hackenberger, E. Smith, S. Dong, D. Viehland, J. Moore, and B. Patrick, *Smart Struct. Mater., Proceeding of SPIE*, 2005, **5761**, 253.
11. K. Kim, S. Zhang, and X. Jiang, *Appl. Phys. Lett.*, 2012, **100**, 253501.
12. X. Jiang, P.W. Rehrig, W.S. Hackenberger, and T. R. Shrout, *Adv. Cryog. Eng.*, 2006, **51A&B**, 1783.
13. D. Damjanovic, *J. Am. Ceram. Soc.*, 2005, **88**, 2663.
14. R. Zhang, B. Jiang, W. Cao, and A. Amin, *J. Mater. Sci. Lett.*, 2002, **21**, 1877.
15. F. Li, S. Zhang, Z. Xu, X, Wei, and T. R. Shrout, *Adv. Funct. Mater.*, 2011, **21**, 2118.
16. S. Zhang, F. Li, J. Luo, R. Sahul, T. R. Shrout, *IEEE Trans. Ultrason. Ferroelectr. Freq. Control*, 2013, **60**, 1572.
17. S. F. Liu, W. Ren, B. K. Mukherjee, S. J. Zhang, T. R. Shrout, P. W. Rehrig and W. S. Hackenberger, *Appl. Phys. Lett.*, 2003, **83**, 2886.
18. J. Jin, K. K. Rajan, and L. Lim, *IEEE Trans. Ultrason. Ferroelectr. Freq. Contr.*, 2007, **54**, 2222.

19. M. Davis, D. Damjanovic, and N. Setter, *J. Appl. Phys.*, 2004, **96**, 2811.

20. Y. X. Tang, X. Y. Zhao, X. Q. Feng, W. Q. Jin, and H. S. Luo, *Appl. Phys. Lett.*, 2005, **86**, 082901.

21. L. Luo, H. Wang, Y. Tang, X. Zhao, Z. Feng, D. Lin, and H. S. Luo, *J. Appl. Phys.*, 2006, **99**, 024104.

22. J. Gao, Z. Xu, F. Li, C. Zhang, Z. Li, X. Wu, L. Wang, Y. Liu, G. Liu, and H. He, *J. Appl. Phys.*, **110**, 2011, 106101.

23. A. Amin, *IEEE Trans. Ultrason. Ferroelectr. Freq. Control.*, 2005, **52**, 1632.

24. Q. Wan, C. Chen, and Y. P. Shen, *J. Appl. Phys.*, 2005, **98**, 024103.

25. D. Viehland, L. Ewart, J. Powers, and J. F. Li, *J. Appl. Phys.*, 2001, **90**, 2479.

26. F. Li, S. Zhang, Z. Xu, D. Lin, J. Gao, Z. Li, and L. Wang, *Appl. Phys. Lett.*, 2012, **100**, 192901.

27. F. Li, S. Zhang, Z. Xu, X. Wei, J. Luo and T. R. Shrout, *Appl. Phys. Lett.*, 2010, **97**, 252903.

28. R. W. Cahn, *Adv. Phys.*, 1954, **3**, 202.

29. J. Fousek and V. Janovec, *J. Appl. Phys.*, 1969, **40**, 135.

30. X. Wang, Z. Xu, Z. Li, and F. Li, *Ferroelectrics*, 2010, **401**, 173.

31. F. Li, L. Jin, Z. Xu, and Z. Guo, *Rev. Sci. Instrum.*, 2009, **80**, 085106.

32. Z. Guo, L. Jin, F. Li, and Y. Bai, *J. Phys. D: Appl. Phys.*, 2009, **42**, 012001.

33. IEEE Standard on Piezoelectricity, "IEEE Standard on Piezoelectricity," ANSI/IEEE Std 176 (1987).

34. R. R. Chien, V. H. Schmidt, C. Tu, and L. W. Hung, H. Luo, *Phys. Rev. B*, 2004, **69**, 172101.

35. C. Jia, K. W. Urban, M. Alexe, D. Hesse, I. Vrejoiu, 2011, *Science*, 2011, **331**, 1420.

36. P. V. Yudin, A.K. Tagantsev, and N. Setter, *Phys. Rev. B*, 2013, **88**, 024102.

37. K. Uchino, J. Zheng, Y. Chen, X. Du, J. Ryu, Y. Gao, S. Ural, S. Priya, and S. Hirose, *J. Mater. Sci.*, 2006, **41**, 217.

38. K. Uchino and S. Hirose, *IEEE Trans. Ultrason. Ferroelectr. Freq. Control*, 2001, **48**, 307.

39. D. Damjanovic and M. Demartin, *J. Phys.: Condens. Matter.*, 1997, **9**, 4943.

40. L. Jin, V. Porokhonskyy, and D. Damjanovic, *Appl. Phys. Lett.*, 2010, **96**, 242902.